

Naval Ocean Systems Center

San Diego, CA 92152-5000



4

DTIC FILE COPY

AD-A223 796

Technical Document 1809

May 1990

Radar Clutter Via Ray Methods

R. A. Pappert

DTIC

SELECTE

JUL 02 1990

D

Approved for public release; distribution is unlimited.

90 06 29 064

NAVAL OCEAN SYSTEMS CENTER
San Diego, California 92152-5000

J. D. FONTANA, CAPT, USN
Commander

R. M. HILLYER
Technical Director

ADMINISTRATIVE INFORMATION

This work was performed by the Ionospheric Branch, Code 542, of the Naval Ocean Systems Center San Diego, CA 92152-5000, with funding provided by the Office of Naval Technology, Arlington, VA 22217, under program element 060243N.

Released by
J. A. Ferguson, Head
Ionospheric Branch

Under authority of
H. J. Richter, Head
Ocean and Atmospheric
Sciences Division

I. INTRODUCTION

In a recent study¹, radar clutter results calculated via waveguide methods were compared with Tappert's* backscatter results generated by using parabolic equation and Monte Carlo methods. For the geometries and environments treated, the waveguide results generally broke down for ranges less than about 8 km. In this study, ray methods along with results of first order scatter theory are used to calculate clutter for ranges applicable to direct illumination, which includes the aforesaid ranges which are inaccessible via waveguide methods. A major question answered in this study is whether any semblance of continuity exists between the ray and waveguide calculations in their region of overlap.

As was the case with the study presented in reference 1, the present development depends heavily upon first order scatter theory from a rough surface as developed by Ulaby, Moore, and Fung². In particular, first order theory is applied to capillary waves on an otherwise flat surface. In actuality the capillary waves ride on long wavelength waves which effect a tilting of the surface, thereby altering the local angle of incidence. Additionally, the long wavelength waves shadow portions of the scattering surface. Awareness of these effects has given rise to the so called "composite surface model" used extensively for within the line of sight calculations in nonconducting environments³⁻⁷. Apart from the horizontal stratification of the media allowed for in the present study, the present development is similar to the line of sight calculations of Chan and Fung⁵ and McDaniel⁷ though no attempt is made here to compare with their radar cross section results.

*This citation refers to a hand-written report prepared by Dr. F. D. Tappert of the University of Miami, while working at NOSC during the summer of 1989. For further information, please contact R. A. Pappert, Code 542, or H. V. Hitney, Code 543, Naval Ocean Systems Center, San Diego, CA.



or	
<input checked="" type="checkbox"/>	
<input type="checkbox"/>	
Distribution/	
Availability Codes	
Dist	Avail and/or Special
A-1	

An outline of the theory for path loss development is given in the following section. Section III contains comparisons of backscatter results obtained via ray, waveguide, and parabolic equation (Tappert) methods at 9.6 GHz for a transmitter at an altitude of 25 m. The results are for the standard atmosphere and evaporation ducts of 14 and 28 m with wind speeds of 10, 20, 30, and 40 knots. Section IV contains concluding remarks.

II. PATH LOSS DEVELOPMENT

Since much of the present section follows the formalism of section II of reference 1, only differences and salient features of the development will be reported here. A rectangular coordinate system is assumed with x the range variable, z the altitude variable with $z = 0$ corresponding to ground level. Horizontal polarization is assumed. The refractive index, assumed to be z dependent, is taken to have unit value at the ground. In actuality, ground values typically correspond to refractivities of several hundred, however translation of the profile is permitted since ray bending depends upon gradients of the refractive index profile. The ground surface is assumed to be rippled, but otherwise flat, with a thin vacuum region immediately above it. Ulaby et al.² have treated, in considerable detail, the problem of first order scatter from such a surface for plane wave incidence. In the high conductivity limit (i.e. $|n_g^2 - 1| \gg S_0^2$), where n_g is the complex ground refractive index and S_0 the sine of the grazing angle of the incident ray, their result for the spectral decomposition of the scattered field due to a unit amplitude incident wave in the x - z plane is (apart from a pulse envelope, a time dependence $\exp(j\omega t)$ is assumed)

$$E_y^{(s)} = -\frac{ik}{2\pi} \int_{-\infty}^{\infty} \int_{-\infty}^{\infty} \int_{-\infty}^{\infty} S_0 z(x', y') \exp(jk_x(x-x') - jk_y y' - jk_z z - jk C_0 x') dk_x dk_y dx' dy', \quad (1)$$

where

$$k = \text{free space wavenumber,} \quad (2)$$

$$S_0 = \text{sine of stationary phase grazing angle,} \quad (3)$$

$$C_0 = \text{cosine of stationary phase grazing angle,} \quad (4)$$

$$k_z = (k^2 - k_x^2 - k_y^2)^{1/2}, \quad (5)$$

$$z(x', y') = \text{random function defining rippled surface.} \quad (6)$$

Unless otherwise specified, MKS units are assumed. Taking $z > 0$ in equation (1), the sign of the square root is taken to assure either upward propagation or evanescence.

The broadside electric field, in the assumed vacuum region bordering the surface, generated by a horizontal electric dipole, \vec{p} , may in the ray approximation be written as⁸

$$E_y^{\text{inc}} = M \frac{(S_0 C_0)^{1/2} \exp(-jkq(\theta_0, x) - jkx C_0)}{(n_T^2 - C_0^2)^{1/4} (x|q''(\theta_0, x)|)^{1/2}}. \quad (7)$$

The new quantities which appear in equation (7) are

$$M = \frac{pk^2}{4\pi\epsilon_0}, \quad \epsilon_0 = \text{free space permittivity,} \quad (8)$$

$$n_T = \text{refractive index at the transmitter height,} \quad (9)$$

$$q(\theta_0, x) = \left| \int_{z_T}^{\infty} (n^2(z) - C_0^2)^{1/2} dz \right| , \quad (10)$$

$$z_T = \text{transmitter height.} \quad (11)$$

The vertical bars in equations (7) and (10) signify absolute values and the double prime on q in equation (7) indicates the second derivative with respect to the grazing angle, θ . The stationary phase angle is determined by the condition

$$x = \frac{1}{\sin \theta} \frac{d}{d\theta} \left| \int_{z_T}^{\infty} (n^2(z) - C^2)^{1/2} dz \right| = 0 . \quad (12)$$

In the present study, the height dependence of the refractive index is approximated by linear segments so that the integral of equation (10) can be evaluated explicitly. For the 14 and 28 m evaporation duct environments used in section III of this study, the linearized descriptions have been given by Hitney.⁹

In accordance with the assumed model, the amplitude of the incident wave in the thin vacuum layer at $z=0$ is simply the quantity which multiplies $\exp(-jkC_0x)$ in equation (7). Inserting this into equation (1) yields

$$E_y^{(s)} = - \frac{jkM}{2\pi^2} \iiint_{-\infty}^{\infty} \frac{S_0(S_0C_0)^{1/2}}{(n_T^2 - C_0^2)^{1/4}} z(x', y') \exp(jk_x(x-x') - jk_y y' - jk_z z) \\ \cdot \frac{1}{(x' | q''(\theta_0, x') |)^{1/2}} \exp(-jkq(\theta_0, x') - jkx'C_0) dk_x dk_y dx' dy' . \quad (13)$$

Using transformations given by equations (22) through (24) and by equations (26) through (28) of reference 1, equation (13) above becomes

$$E_y^{(s)} = -\frac{jk^3 M}{2\pi} \int_{-\infty}^{\infty} \int_{-\infty}^{\infty} dx' dy' \frac{S_o (S_o C_o)^{1/2} z(x', y')}{(n_T^2 - C_o^2)^{1/4} (x' |q''(\theta_o, x')|)^{1/2}} \cdot \int_{-j\infty}^{j\infty} S H_o^{(2)}(krC) \exp(-jkzS) d\theta, \quad (14)$$

where $H_o^{(2)}$ is the Hankel function of order zero of the second kind and $r = (x-x')^2 + y'^2)^{1/2}$. Taking $x=0$, r will be approximated by x' , which seems reasonable for beam widths much less than one radian.

When multiplied by the factor, $-jk/2$, the integral over θ in equation (14), apart from the factor S , is simply the free space Green's function for scatter to the point (x, z) with z in the assumed vacuum region bordering the surface. Thus, for a horizontally stratified environment, the following replacement for backscatter (i.e. $x = 0$, $z = z_T$) applies in the asymptotic limit $kx' \gg 1$

$$-\frac{jk}{2} \int_{-j\infty}^{j\infty} S H_o^{(2)}(kx'C) \exp(-jkzS) d\theta \rightarrow \frac{S_o (S_o C_o)^{1/2} \exp(-jkq(\theta_o, x') - jkx'C_o)}{(n_T^2 - C_o^2)^{1/4} (x' |q''(\theta_o, x')|)^{1/2}}. \quad (15)$$

Making this replacement in equation (14) yields

$$E_y^{(s)} = \frac{k^2 M}{\pi} \int_{-\infty}^{\infty} \int_{-\infty}^{\infty} dx' dy' \frac{S_o^3 C_o z(x', y')}{(n_T^2 - C_o^2)^{1/2} x' |q''(\theta_o, x')|} \exp(-2jkq(\theta_o, x') - 2jkx'C_o). \quad (16)$$

Since

$$H_z^{(s)} \approx \frac{k^2 M}{\pi \eta} \iint dx' dy' \frac{S_o^3 C_o^2 z(x', y')}{(n_T^2 - C_o^2)^{1/2} x' |q''(\theta_o, x')|} \exp(-2jkq(\theta_o, x') - 2jkx' C_o), \quad (17)$$

where η is the free space impedance, the Poynting flux associated with the scattered field is

$$\begin{aligned} \frac{1}{2} \text{Re} \langle E_y^{(s)} H_z^{(s)*} \rangle_\infty &= \frac{1}{2\eta} \frac{k^4 M^2}{\pi^2} \text{Re} \iiint_{-\infty}^{\infty} dx' dy' dx'' dy'' \\ &\cdot \frac{S_o^3(x') S_o^3(x'') C_o^2(x') C_o^2(x'') \langle z(x', y') z(x'', y'') \rangle}{(n_T^2 - C_o^2(x'))^{1/2} (n_T^2 - C_o^2(x''))^{1/2} x' x'' |q''(\theta_o(x'), x')| |q''(\theta_o(x''), x'')|} \\ &\cdot \exp(-2jk(q(\theta_o(x'), x') - q(\theta_o(x''), x'')) - 2jk(C_o(x')x' - C_o(x'')x''))), \end{aligned} \quad (18)$$

where the explicit dependence of S_o , C_o , θ_o on range has been indicated and where the braces, $\langle \rangle$, denote an ensemble average.

Next let

$$\bar{x} = x' - x'', \quad \bar{y} = y' - y'', \quad X = \frac{1}{2}(x' + x''), \quad Y = \frac{1}{2}(y' + y''), \quad (19)$$

$$dx' dy' dx'' dy'' = d\bar{x} d\bar{y} dX dY. \quad (20)$$

Assuming $z(x', y')$ is a homogeneous random function, the ensemble average $\langle z(x', y') z(x'', y'') \rangle$ simply becomes $\rho(\bar{x}, \bar{y})$ where ρ is the surface correlation function. Because $C_o = 1$ and since significant contribution to the \bar{x} integral comes only from distances on the order of the surface correlation length (i.e. on the order of centimeters), equation (18) may be approximated as follows:

$$\frac{1}{2} \text{Re} \langle E_y^{(s)} H_z^{(s)*} \rangle \approx - \frac{k_M^2}{2\eta\pi^2} \text{Re} \iiint_{-\infty}^{\infty} dX dY d\bar{X} d\bar{Y} \frac{S_o^4(X) \rho(\bar{X}, \bar{Y}) \exp(-2jk\bar{X})}{(n_T^2 - C_o^2(X)) X^2 |g''(\theta_o(X), X)|^2}, \quad (21)$$

where

$$g''(\theta_o(X), X) = q''(\theta_o(X), X) / S_o(X). \quad (22)$$

Using the spectrum relationship

$$2\pi w(k_x, k_y) = \iint_{-\infty}^{\infty} \rho(\bar{X}, \bar{Y}) \exp(-jk_x \bar{X} - jk_y \bar{Y}) d\bar{X} d\bar{Y}, \quad (23)$$

equation (21) transforms to

$$\frac{1}{2} \text{Re} \langle E_y^{(s)} H_z^{(s)*} \rangle \approx - \frac{k_M^2}{\eta\pi} w(2k, 0) \iint_{-\infty}^{\infty} dX dY \frac{S_o^4(X)}{(n_T^2 - C_o^2(X)) X^2 |g''(\theta_o(X), X)|^2}. \quad (24)$$

It is next assumed that the integrand is sufficiently constant over the illuminated area so that,

$$\int f(x) dx \approx \Delta X f(x), \quad (25)$$

where ΔX is the pulse length and X the range to the midpoint of the illuminated area. The final integral reduction of equation (24) is made by replacing dY by $X d\phi$ and by assuming a Gaussian azimuthal beam pattern with a 3 dB half width, ϕ_o . Subject to these assumptions, equation (24) becomes

$$\frac{1}{2} \text{Re} \langle E_y^{(s)} H_z^{(s)*} \rangle \approx - \frac{k^4 M^2}{\eta \pi} \left(\frac{\pi}{\ln 2} \right)^{1/2} \phi_o w(2k, o) \frac{\Delta X}{X} \frac{S_o^4}{(n_T^2 - C_o^2) |g''(\theta_o)|^2}, \quad (26)$$

where ϕ_o is in radians and the explicit dependency of S_o , C_o , and θ_o on X has been dropped. The minus sign in equation (26) simply signifies propagation in the negative x direction and is dropped from this point on. To convert to path loss equation (26), as discussed in reference 1, is multiplied by the factor

$$\frac{\pi}{k^2} \frac{2}{3} \frac{3\eta}{4\pi k^2} \left(\frac{4\pi\epsilon_o}{p} \right)^2, \quad (27)$$

thereby giving

$$PL(\text{dB}) \approx -10 \log_{10} \left\{ 1.486 \times 10^2 f_{gh}^2 \phi_o w(2k, o) \frac{\theta_o^4 \Delta X}{X(n_T^2 - C_o^2) |g''(\theta_o)|^2} \right\}. \quad (28)$$

Note that in equation (28) the replacement $S_o \approx \theta_o$ has been made. Also, f_{gh} is the frequency in GHz. The spectrum function $w(k_x, k_y)$ equals $w_p(k)/k$ where $k = (k_x^2 + k_y^2)^{1/2}$ and w_p is the Pierson spectrum.¹⁰

Long surface wavelength effects are allowed for by first multiplying the argument of the logarithm of equation (28) by the Wagner shadowing function¹¹, $G(\theta_o)$, as discussed in reference 1. Next, surface tilting effects are approximately allowed for by replacing θ_o in the numerator of equation (28) by

$(\theta_o + (\overline{\eta^4})_{il}^{1/4})$ where $(\overline{\eta^4})_{il}$ is the fourth power of the long wavelength sea surface slope averaged over the unshadowed portion of the surface. This averaging could be improved upon but is adequate for the examples considered

for which $\theta_o \leq 2 \times 10^{-2}$ rad and $(\eta^4)_{il}^{1/4} \geq 0.13$ rad. Calculation of $(\eta^4)_{il}$ is discussed in references 1 and 11.

Including the long surface wavelength effects in equation (28) via the methods just described gives,

$$PL(dB) \approx -10 \log_{10} \left\{ 1.486 \times 10^2 f_{gh}^2 \phi_o w(2k, o) G(\theta_o) \frac{(\theta_o + (\eta^4)_{il}^{1/4})^4 \Delta X}{X(n_T^2 - C_o^2) |g''(\theta_o)|^2} \right\} . \quad (29)$$

III RESULTS

Based on a parabolic equation method, Tappert has given backscatter results for a single surface realization for the standard atmosphere and for two evaporation ducts. The latter were characterized by duct heights of 14 and 28 m and have been described by Hitney.⁹ Tappert's calculations apply to a frequency of 9.6 GHz, a transmitter height of 25 m, a pulse width of 1.0 μs (in our convention $\Delta X = c\tau/2$ with c the speed of light and τ pulse width) and a 3 dB full beam width of 1.2°. Results for wind speeds of 10, 20, 30, and 40 knots were given. In a subsequent study,¹ waveguide calculations for the average backscatter levels were compared with Tappert's results. Those comparisons indicated reasonable agreement for the average fields for the ducted cases for ranges beyond about 8 km. At shorter ranges the waveguide results broke down. In the nonducting cases, that is the standard atmosphere cases, the waveguide results were about 10 dB high relative to the parabolic equation results. This did not seem surprising since the application of shadowing notions used in conjunction with waveguide concepts were most suspect for the standard atmosphere cases because the dominant mode is evanescent at the ground. That is to say, the real part of the eigenangle for the dominant mode is 8.06×10^{-4} rad while the imaginary part is 1.40×10^{-3} rad. This can be

contrasted with the ducting cases. The real part of the eigenangle for the dominant mode for the 14 m duct is about 4.75×10^{-3} rad for the four windspeeds and the imaginary parts are less than 4×10^{-5} rad for the four windspeeds. For the 28 m duct, the real part of the eigenangle for the dominant mode is about 7×10^{-3} rad and the imaginary parts are less than 3×10^{-5} rad for the four wind speeds. Thus, ray notions such as shadowing are eminently more reasonable for the ducting environments.

In the present study, the above comparisons are supplemented with calculations based entirely upon ray concepts as discussed in section II. Figures 1 through 4 show comparisons of the three methods for the standard atmosphere and the four wind speeds. Ray results for the average backscatter agree well with the parabolic equation results out to ranges between about 5 and 10 km depending upon wind speed. They generally intersect the waveguide results at ranges slightly in excess of 10 km and give larger results than the other two methods beyond there and out to the horizon (≈ 20.6 km). It is not absolutely clear which results are to be believed. However, as mentioned above, the waveguide calculations are suspect in the standard atmosphere case. On the other hand, the parabolic equation results have no range or profile limitation and exhibit the greatest degree of continuity for the average field. It will, therefore, be assumed that the parabolic equation results are to be preferred. Failure of ray theory is expected as the shadow boundary is approached. However, it is not known to the author whether or not, for the conditions of figures 1 through 4, that failure would be expected to occur more than 10 km from the shadow boundary. Clearly a criterion is needed to establish the region of validity of the ray theory. If such a criterion indicated ray failure only for ranges closer to the horizon, then, the most likely explanation for the calculated onset of ray theory departure from the parabolic equation results would be failure of the shadowing theory.

The rapid change in signal level close to the horizon, which is evident in figures 1 through 4, may be traced to a rapid decrease in the relative value of the grazing angle (and concomitant decrease in the shadowing function) as the horizon is approached.

As a typical case, figure 5 shows path loss comparisons between the ray and waveguide methods for the 14 m duct with a 20 knot wind. In this case the extended radio horizon is about 61 km and the waveguide calculation should be valid beyond about 5 km. As figure 5 shows, departure between the two calculations sets in at about 40 km. Again, it is not known why departure of the ray calculation from the waveguide calculation begins so far (≈ 20 km) from the radio horizon. (Nevertheless, there is clearly a large range, ≈ 40 km, over which ray theory gives acceptable results).

Figures 6 through 9 show comparisons of the three methods for the 14 m duct and the four wind speeds. Unlike figure 5, the range axis only extends to 40 km. In all cases, average fields determined by the three methods agree to better than 10 dB over their regions of validity.

As a representative case, figure 10 shows path loss comparisons between the ray and waveguide methods for the 28 m duct with a 20 knot wind. In this case, the extended radio horizon is about 81 km and the waveguide calculation should be valid beyond about 5 km. As was the case with the 14 m duct, departure between the two calculations sets in at about 40 km. For ranges less than that the two methods agree quite well in their overlapping regions of validity. As with the 14 m duct, it is not known why departure of the ray calculation from the waveguide calculation begins so far (≈ 40 km) from the shadow boundary.

As an academic curiosity, there is a modal interference null at about 68 km indicated in the waveguide result. It would be interesting to know if a comparable null showed up in the parabolic equation method.

Figures 11 through 14 show comparisons of the three methods for the 28 m duct and the four wind speeds. Unlike figure 10, the range axis only extends to 40 km. In all cases, average fields determined by the three methods agree to better than 10 dB over their range of validity.

IV DISCUSSION

In this study, backscatter results based on ray theory have been generated at 9.6 GHz for a transmitter altitude of 25 m. The standard atmosphere along with evaporation ducts of 14 and 28 m have been considered for wind speeds of 10, 20, 30, and 40 knots. Only horizontal polarization has been considered in the high conductivity limit. Expectations are that vertical polarization would behave in a similar fashion in this limit, though this should be checked.

Ray theory results for the average clutter power have been compared with parabolic equation results of Tappert and waveguide results of an earlier study.¹ Unlike the parabolic equation method, the ray and waveguide calculations, based on first order scatter theory, yield only estimates of the average clutter power. The parabolic equation method also yields estimates for the variance of the backscatter power. Higher order scatter theory is required to estimate variances via ray or waveguide models. Average clutter powers via ray and waveguide models have been calculated using the Pierson sea spectrum while the parabolic equation results of Tappert were obtained using a different spectrum.

Ray and parabolic equation results for the standard atmosphere agree out to ranges between 5 and 10 km depending upon windspeed. In these cases the ray and waveguide results do not continuously blend into each other. Comparison of the three methods for the 14 and 28 m ducting environments indicates agreement to better than 10 dB over a 40 km range (waveguide results

break down for ranges less than about 8 km - the other methods are not restricted by this limitation). Ray calculations, of course, require less cpu time than the other two methods. However, a criterion for validity of the ray method, as the shadow boundary is approached, is needed.

Further comparisons of the methods should be made along with comparisons with experimental data. Since there are many dB uncertainties in the sea spectrum values, it is likely that constants or correction factors can be determined empirically to yield best results with the latter.

Acknowledgement: The author wishes to thank Ms. L. R. Hitney for programming assistance.

REFERENCES

1. Pappert, R.A. 1989. "Radar Clutter via Waveguide Methods." NOSC TD 1739 (Dec), Naval Ocean Systems Center, San Diego, CA.
2. Ulaby, F.T., R.K. Moore and A.K. Fung. 1982. Microwave Remote Sensing Active and Passive, Vol II: Radar Remote Sensing and Surface Scattering and Emission Theory, Addison-Wesley Publishing Co., London, England.
3. Fung, A.K. and H.L. Chan. 1969. "Backscattering of Waves by Composite Rough Surfaces", IEEE Trans. Antennas and Propagation, AP-17, pp 590-597.
4. Peake, W.H., D.L. Barrick, A.K. Fung and H.L. Chan. 1970. "Comments on Backscattering of Waves by Composite Rough Surfaces", IEEE Trans. Antennas and Propagation", AP-18, pp 716-728.
5. Chan, H.L. and A.K. Fung. 1977. "A Theory of Sea Scatter at Large Incidence Angles", Jour. Geophys. Res., Vol 82, No. 24, pp 3439-3444.
6. Bass, F.G. and I.M. Fuks. 1979. Wave Scattering from Statistically Rough Surfaces, Pergamon Press, New York, N.Y.
7. McDaniel, S.T. and A.D. Gorman. 1982. "Acoustic and Radar Sea Surface Backscatter", Jour. Geophys. Res., Vol. 87, No. C6, pp 4127-4136.
8. Brekhovskikh, L.M. 1980. Waves in Layered Media, 2nd Edition, Academic Press, New York, N.Y.
9. Hitney, H.V. 1988. "Evaporation Duct Effects on Low Altitude Propagation", NOSC TR 1304 (June), Naval Ocean Systems Center, San Diego, CA.

10. Pierson, W.J. 1976. "The Theory and Applications of Ocean Wave Measuring Systems at and Below-Sea Surface on the Land, from Aircraft and from Spacecraft", NASA Contract Rep. CR-2646, NASA, Washington, DC.

11. Wagner, R.J. 1967. "Shadowing of Randomly Rough Surfaces", Jour. Acous. Soc. Amer., Vol 41, No. 1, pp 138-147.

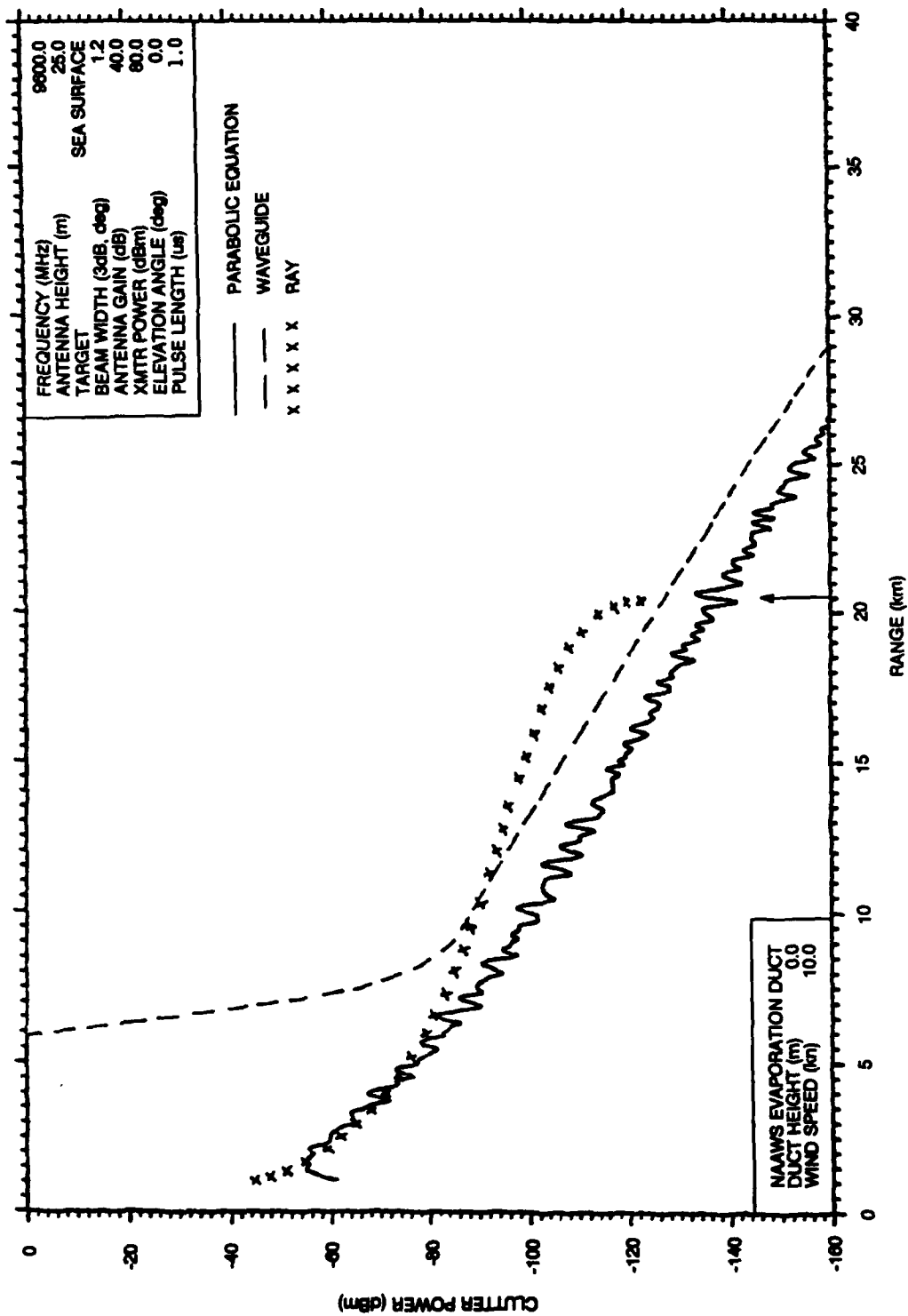


Figure 1. Clutter power vs. range. Comparison between pe, waveguide and ray results.
 Standard atmosphere, 10 knot wind.

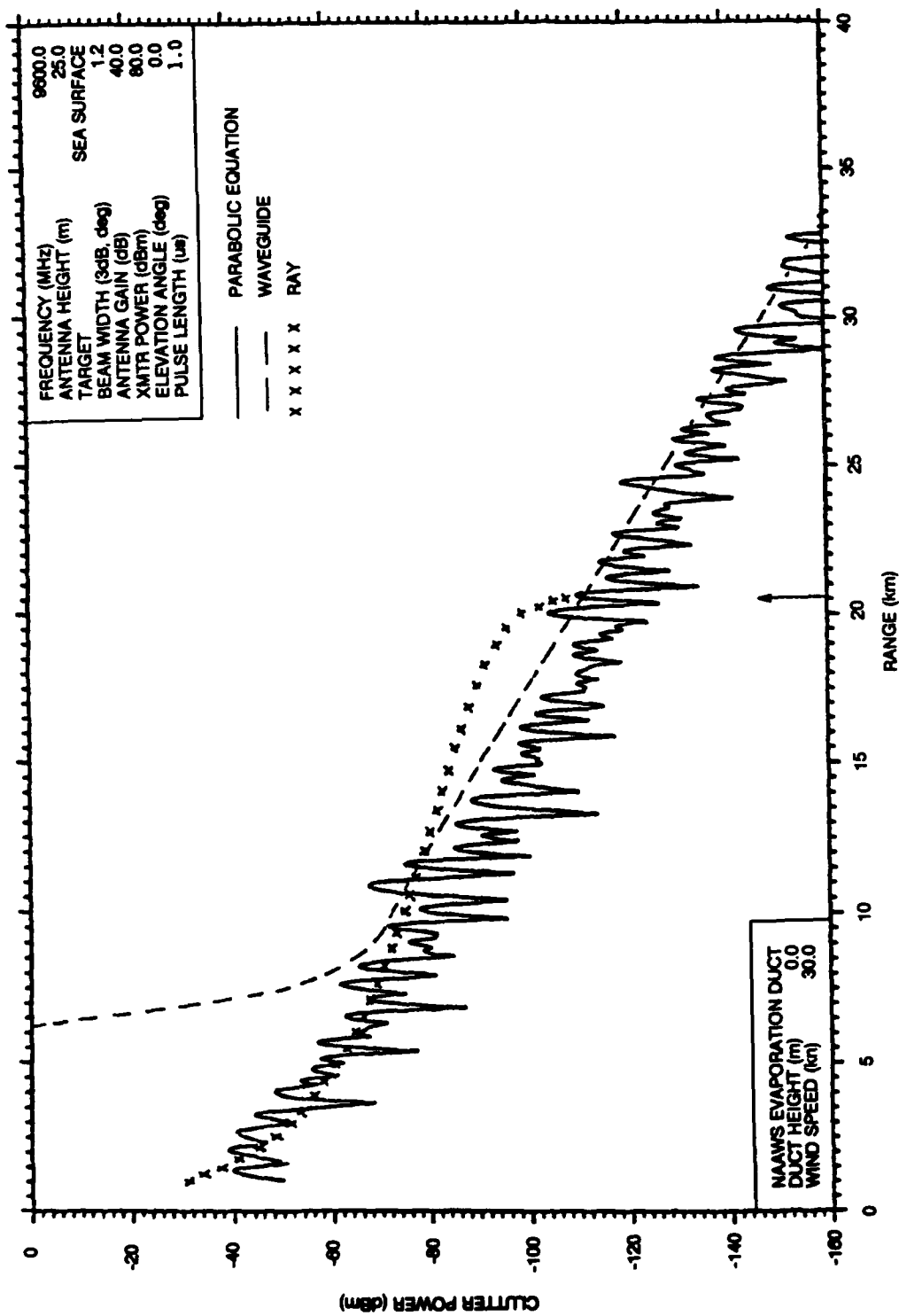


Figure 3. Clutter power vs. range. Comparison between pe, waveguide and ray results.
Standard atmosphere, 30 knot wind.

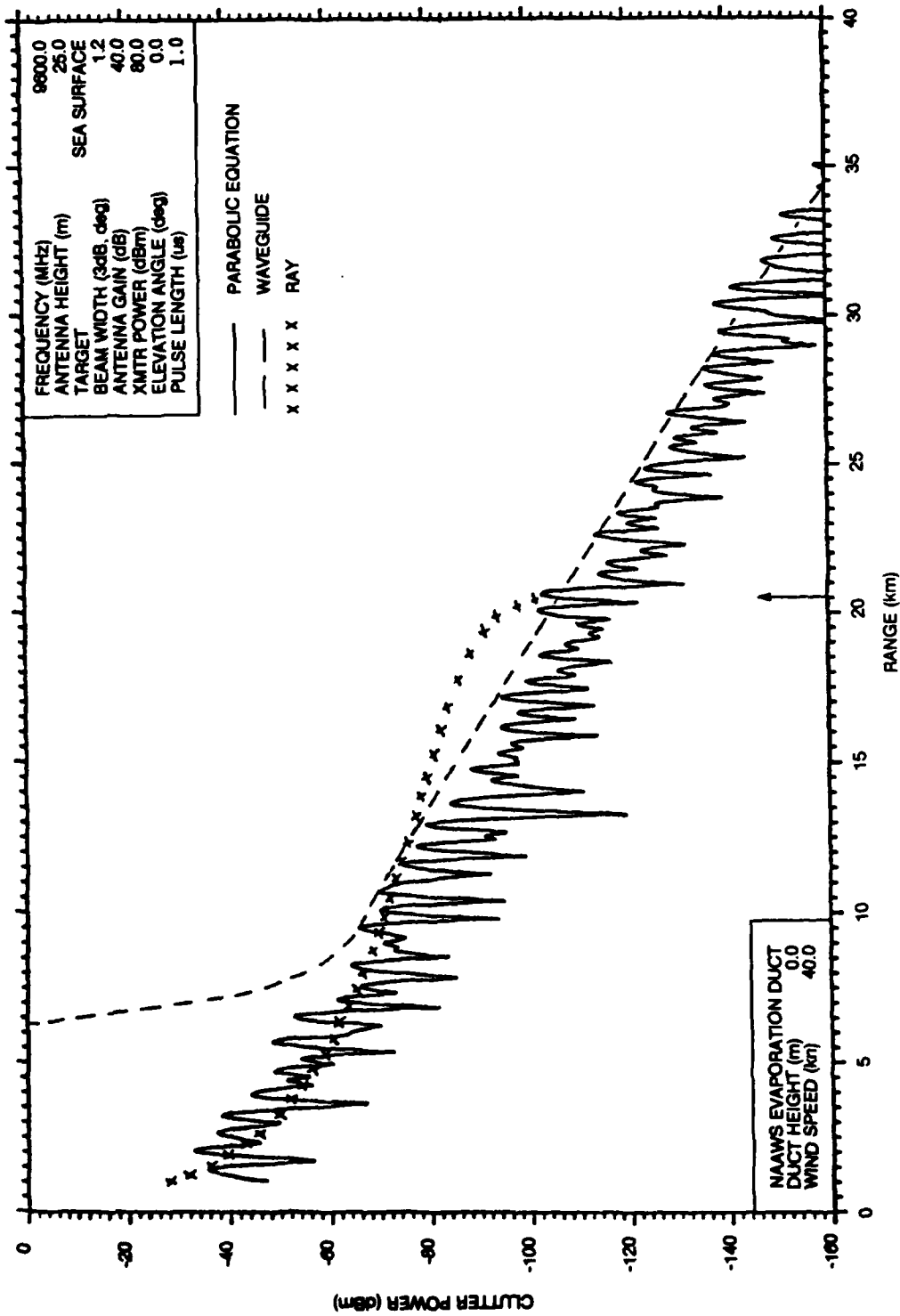


Figure 4. Clutter power vs. range. Comparison between pe, waveguide and ray results. Standard atmosphere, 40 knot wind.

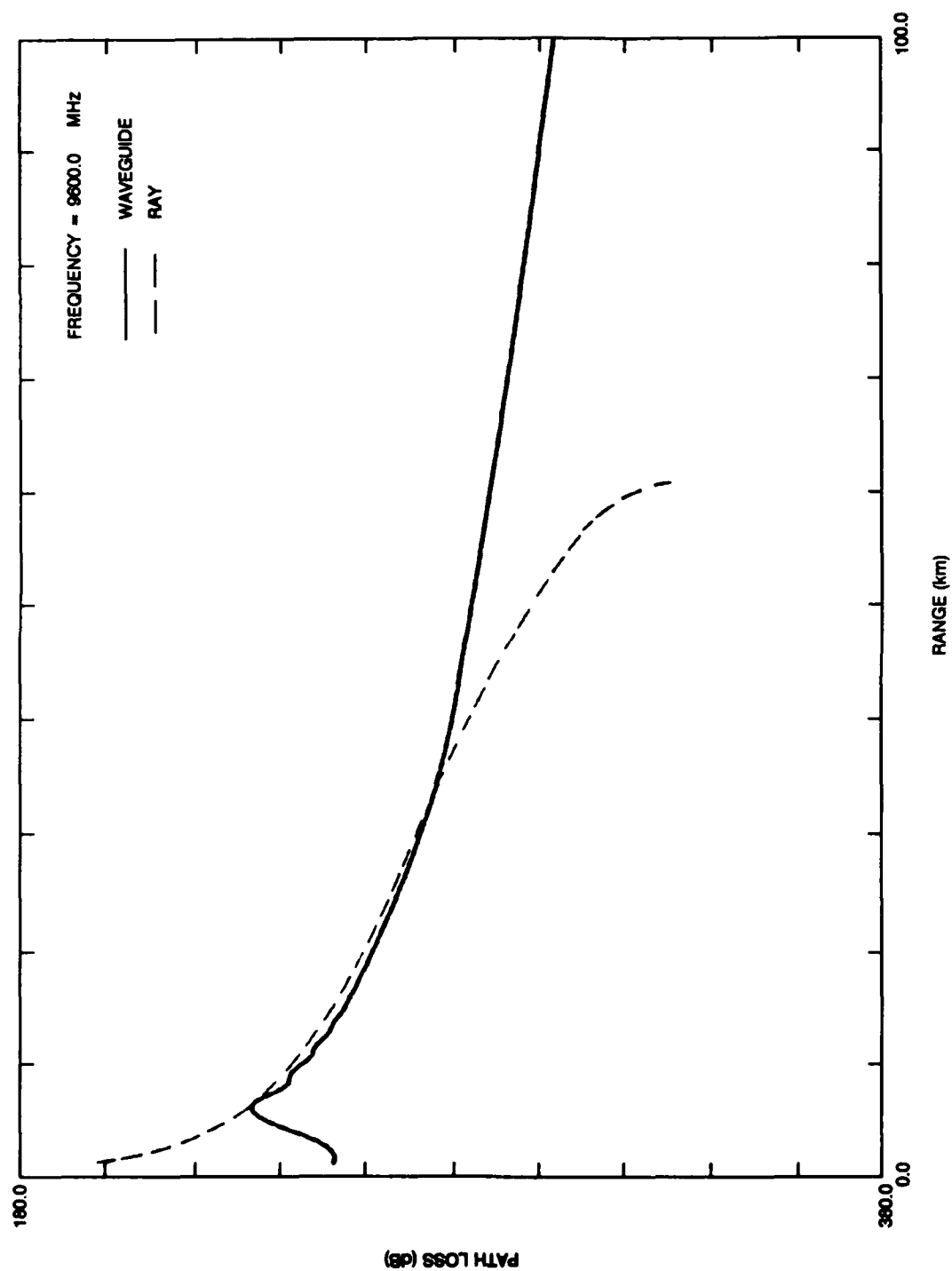


Figure 5. Path loss vs. range for a 14m evaporation duct. Comparison between ray and waveguide results. Transmitter-receiver height of 25m and 20 knot wind.

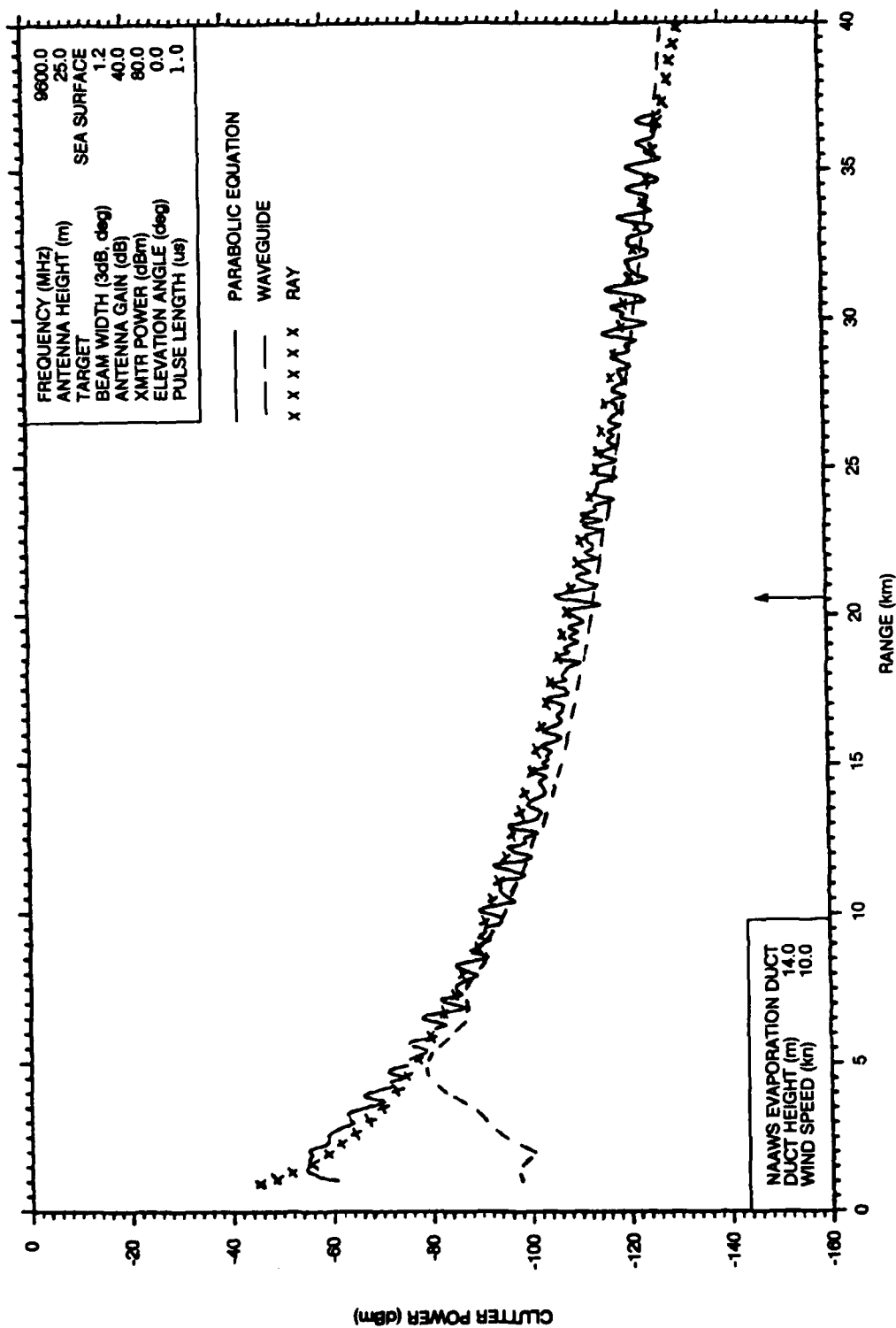


Figure 6. Clutter power vs. range. Comparison between pe, waveguide and ray results.
 Fourteen meter evaporation duct, 10 knot wind.

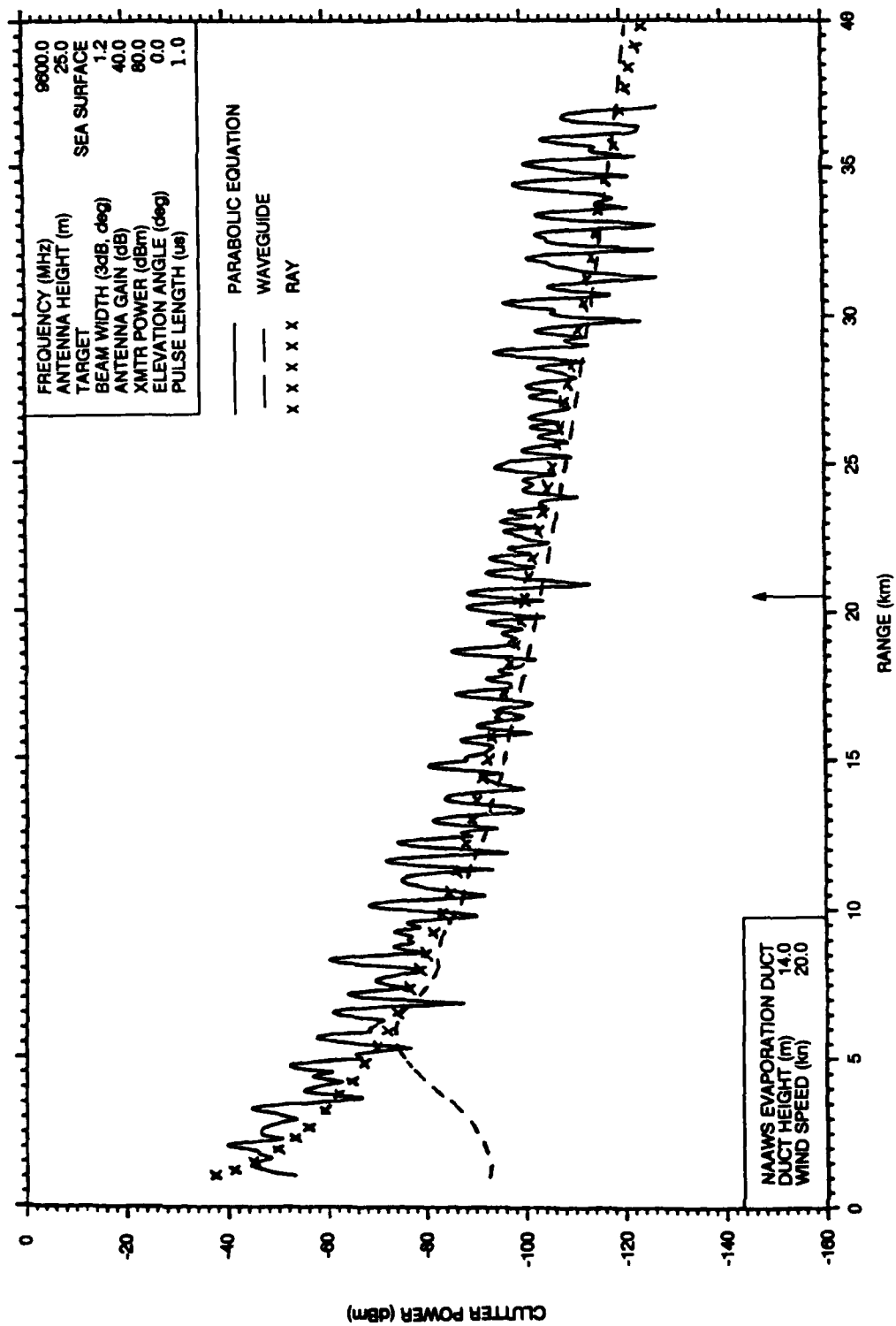


Figure 7. Clutter power vs. range. Comparison between pe, waveguide and ray results. Fourteen meter evaporation duct, 20 knot wind.

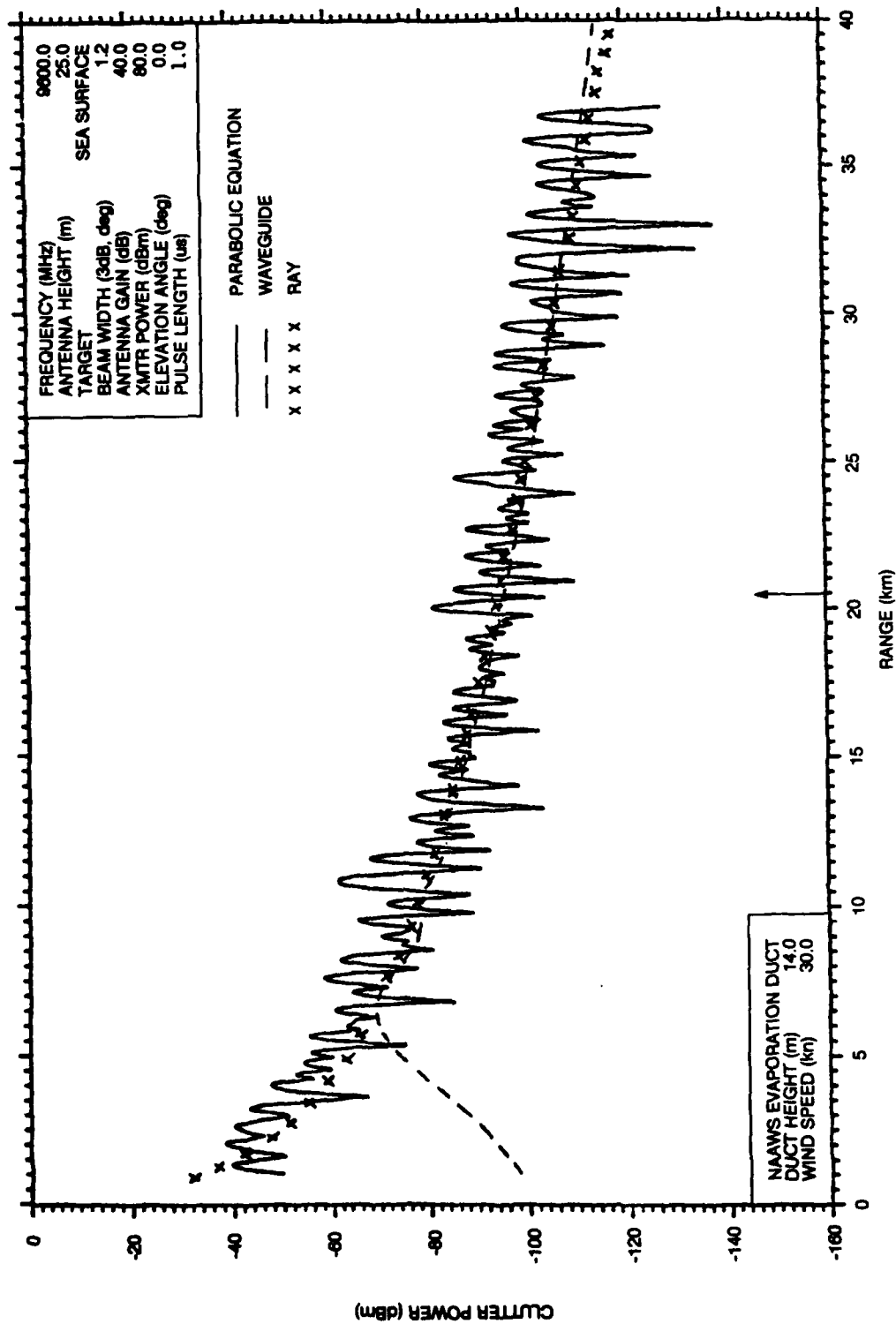


Figure 8. Clutter power vs. range. Comparison between pe, waveguide and ray results.
Fourteen meter evaporation duct, 30 knot wind.

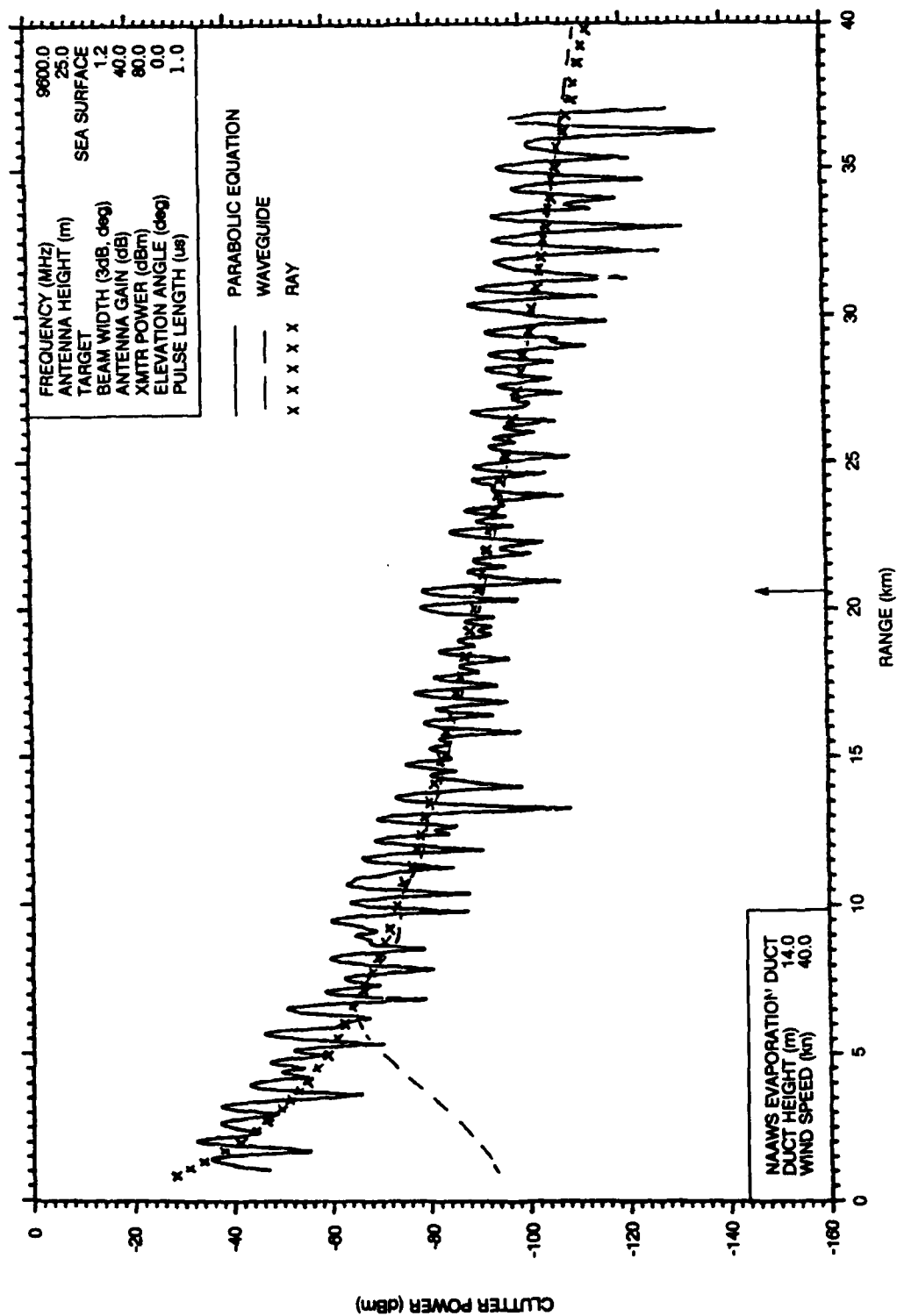


Figure 9. Clutter power vs. range. Comparison between pe, waveguide and ray results. Fourteen meter evaporation duct, 40 knot wind.

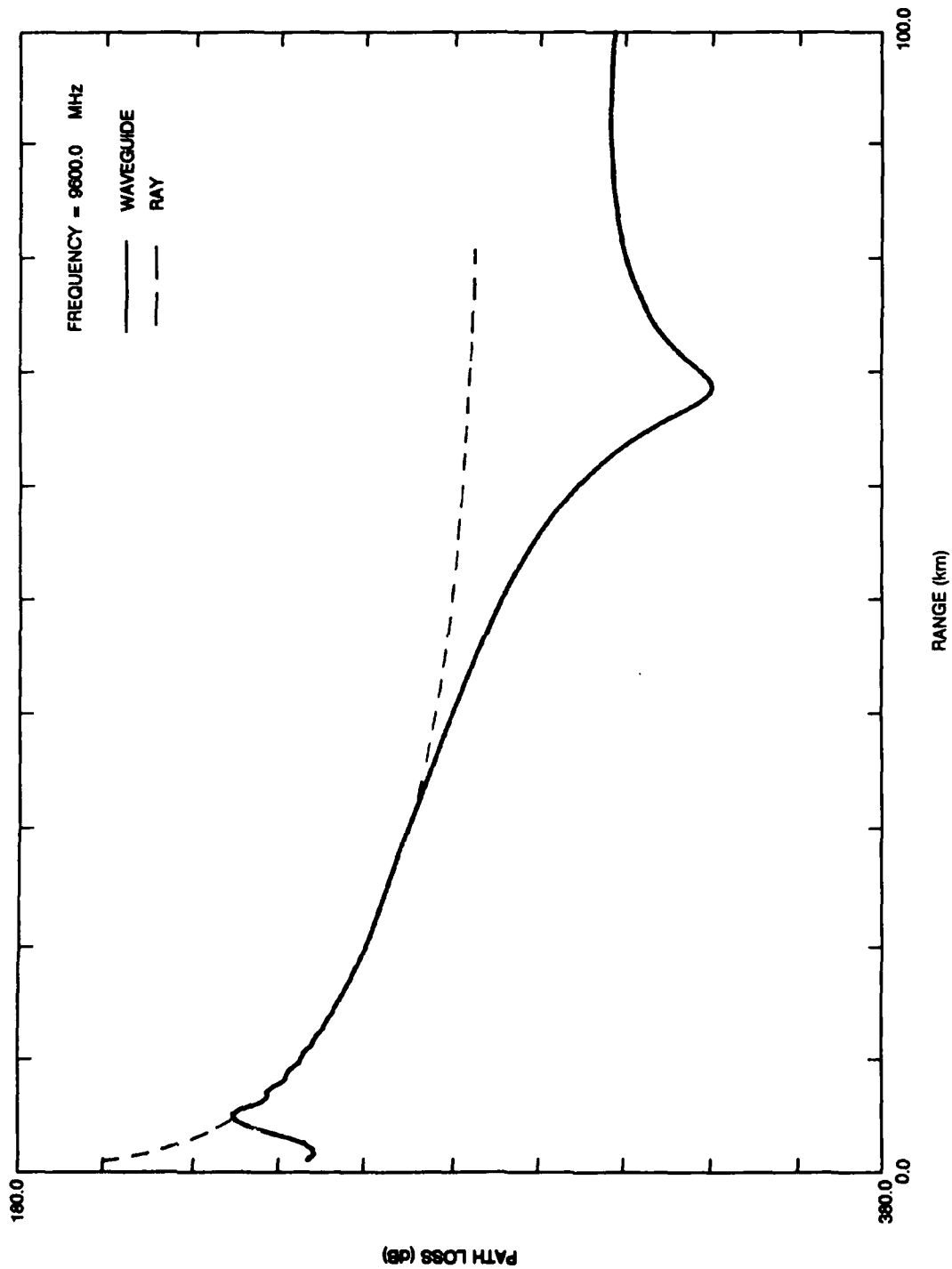


Figure 10. Path loss vs. range for a 28m evaporation duct. Comparison between ray and waveguide results. Transmitter-receiver height of 25m and 20 knot wind.

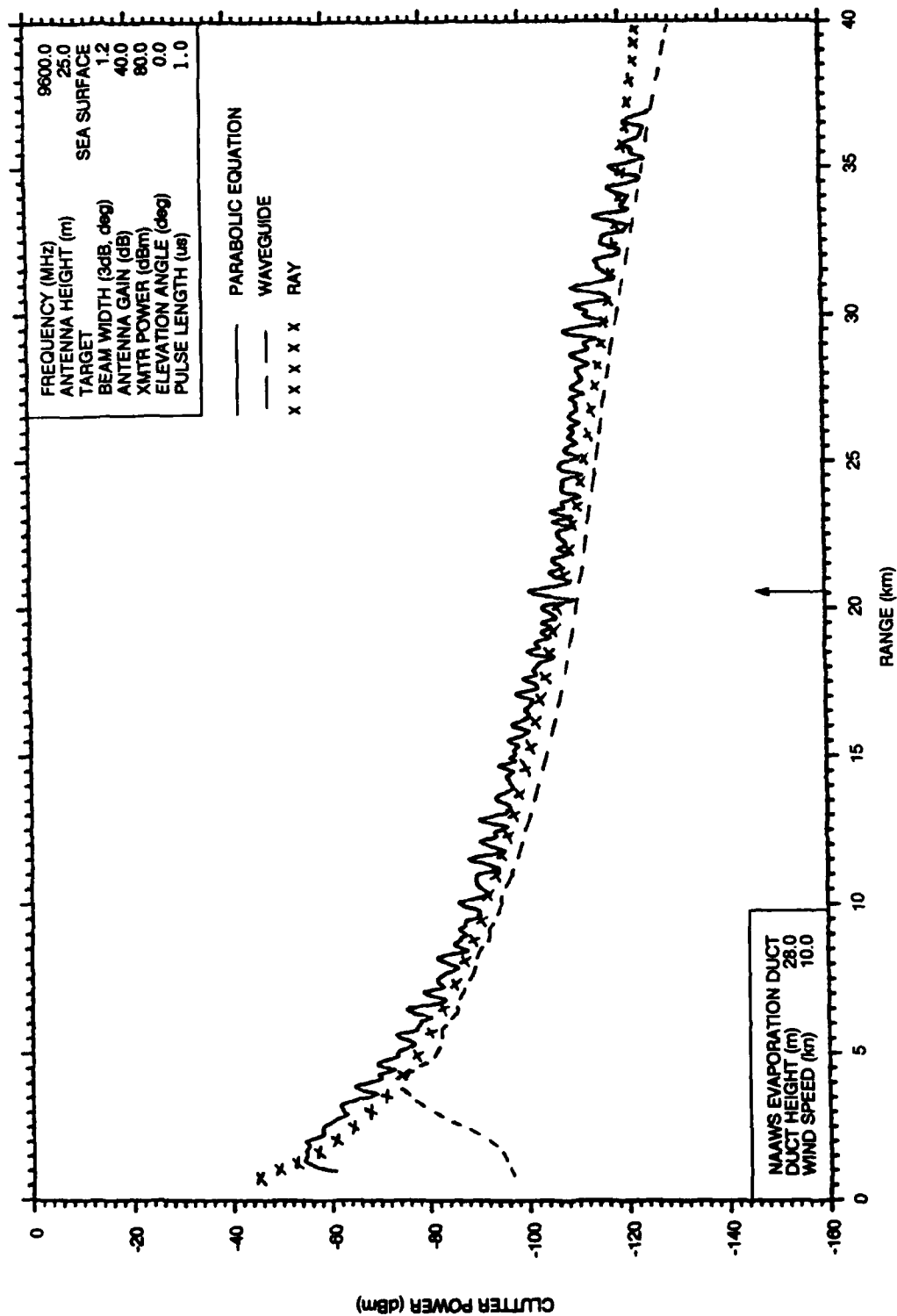


Figure 11. Clutter power vs. range. Comparison between pe, waveguide and ray results.
 Twenty eight meter evaporation duct, 10 knot wind.

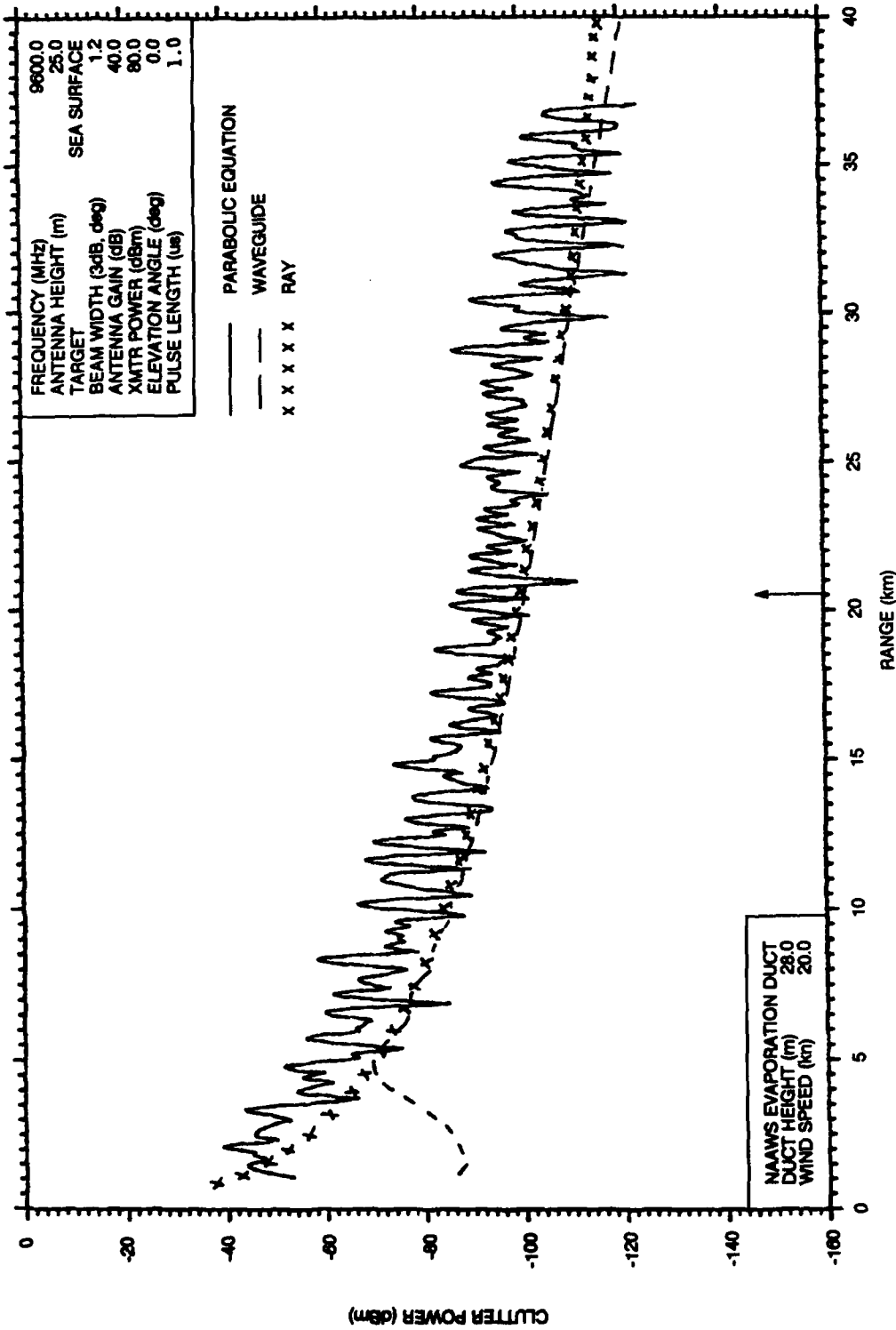


Figure 12. Clutter power vs. range. Comparison between pe, waveguide and ray results. Twenty eight meter evaporation duct, 20 knot wind.

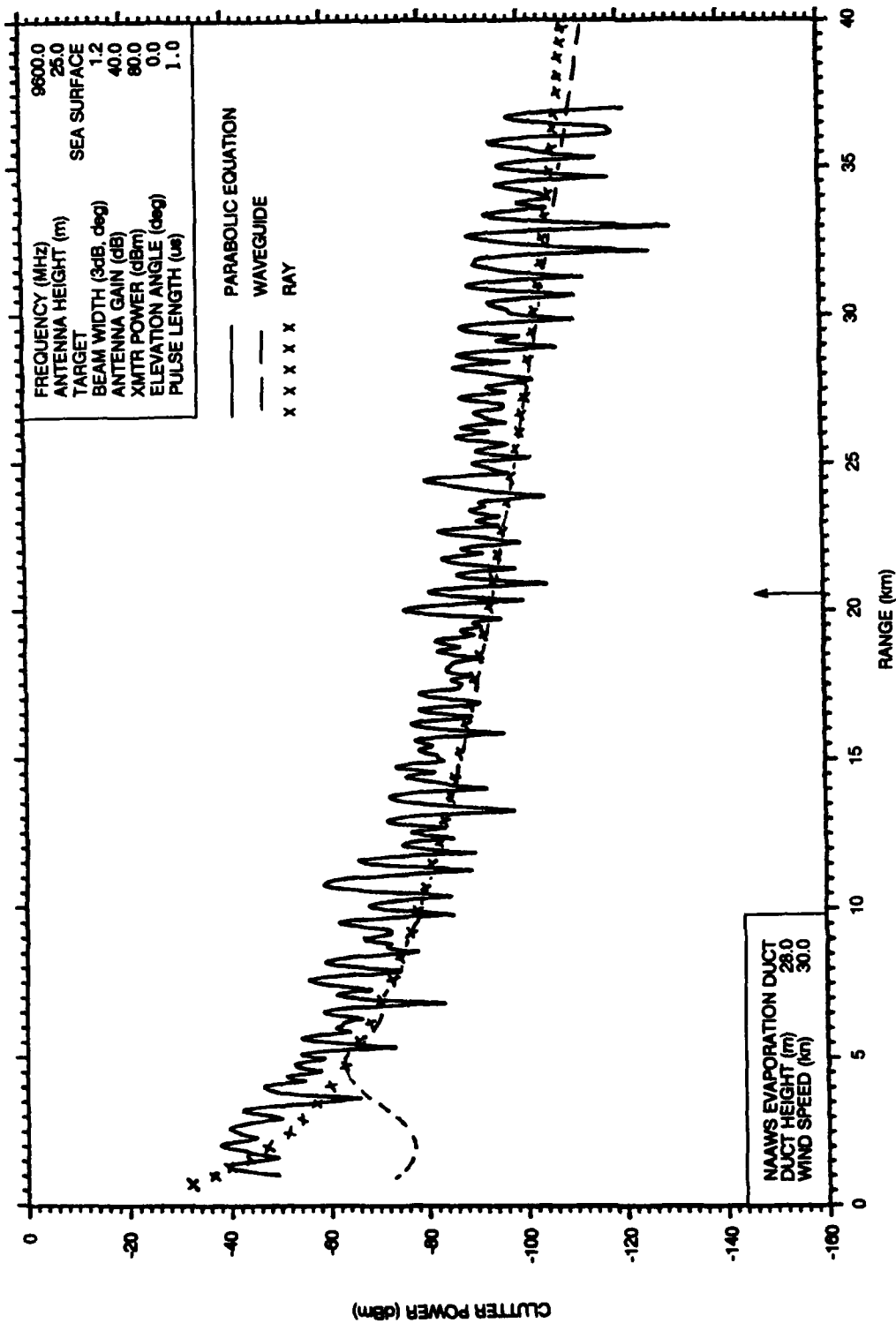


Figure 13. Clutter power vs. range. Comparison between pe, waveguide and ray results.
Twenty eight meter evaporation duct, 30 knot wind.

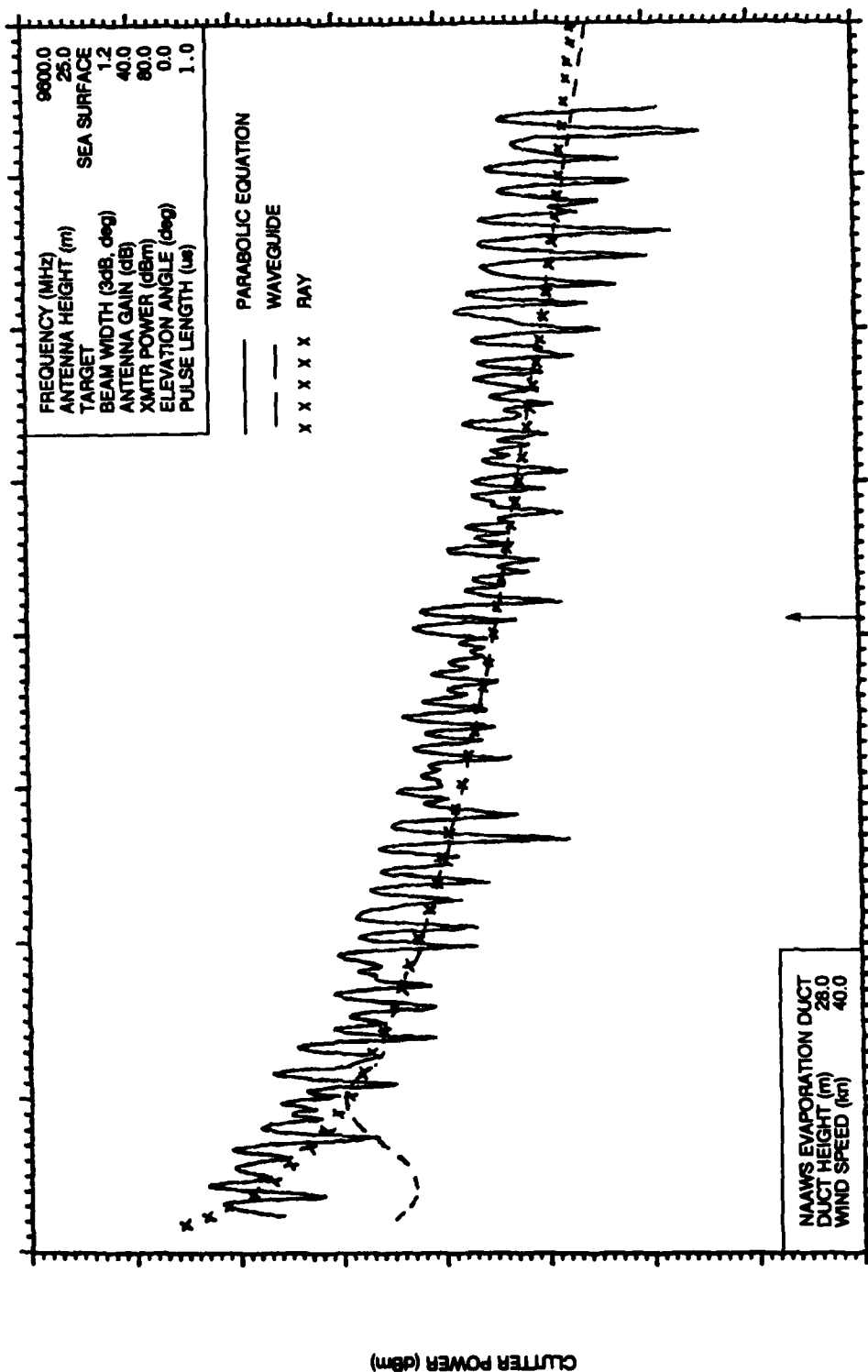


Figure 14. Clutter power vs. range. Comparison between pe, waveguide and ray results.
Twenty eight meter evaporation duct, 40 knot wind.

REPORT DOCUMENTATION PAGE

Form Approved
OMB No. 0704-0188

Public reporting burden for this collection of information is estimated to average 1 hour per response, including the time for reviewing instructions, searching existing data sources, gathering and maintaining the data needed, and completing and reviewing the collection of information. Send comments regarding this burden estimate or any other aspect of this collection of information, including suggestions for reducing this burden, to Washington Headquarters Services, Directorate for Information Operations and Reports, 1215 Jefferson Davis Highway, Suite 1204, Arlington, VA 22202-4302, and to the Office of Management and Budget, Paperwork Reduction Project (0704-0188), Washington, DC 20503.

1. AGENCY USE ONLY (Leave blank)		2. REPORT DATE May 1990	3. REPORT TYPE AND DATES COVERED Final
4. TITLE AND SUBTITLE RADAR CLUTTER VIA RAY METHODS		5. FUNDING NUMBERS PE: 0602435N WU: DN488 760	
6. AUTHOR(S) R. A. Pappert			
7. PERFORMING ORGANIZATION NAME(S) AND ADDRESS(ES) Naval Ocean Systems Center San Diego, CA 92152-5000		8. PERFORMING ORGANIZATION REPORT NUMBER NOSC TD 1809	
9. SPONSORING/MONITORING AGENCY NAME(S) AND ADDRESS(ES) Office of Naval Technology Arlington, VA 22217		10. SPONSORING/MONITORING AGENCY REPORT NUMBER	
11. SUPPLEMENTARY NOTES			
12a. DISTRIBUTION/AVAILABILITY STATEMENT Approved for public release; distribution is unlimited.		12b. DISTRIBUTION CODE	
13. ABSTRACT (Maximum 200 words) In a recent study, radar clutter results calculated via waveguide methods were compared with Tappert's backscatter results generated by using parabolic equation and Monte Carlo methods. For the geometries and environments considered, the waveguide results generally broke down for ranges less than about 8 km. In this study, ray methods, along with results of first order scatter theory, are used to calculate clutter for ranges applicable to direct illumination. The latter includes those close in ranges not accessible via waveguide methods. Ray theory comparisons with Tappert's results and waveguide results are given at 9.6 GHz for the standard atmosphere, and for 14 and 28 m evaporation ducts. Results apply to wind speeds of 10, 20, 30, and 40 knots at a transmitter altitude of 25 m. <i>8 km</i> <i>25 m</i> <i>Kilometers</i>			
14. SUBJECT TERMS Waveguide methods, radar clutter, <i>Active and Passive Radar Detection and</i> <i>Equipment, Ray Methods</i>		15. NUMBER OF PAGES 33	
17. SECURITY CLASSIFICATION OF REPORT UNCLASSIFIED		18. SECURITY CLASSIFICATION OF THIS PAGE UNCLASSIFIED	
19. SECURITY CLASSIFICATION OF ABSTRACT UNCLASSIFIED		20. LIMITATION OF ABSTRACT SAME AS REPORT	